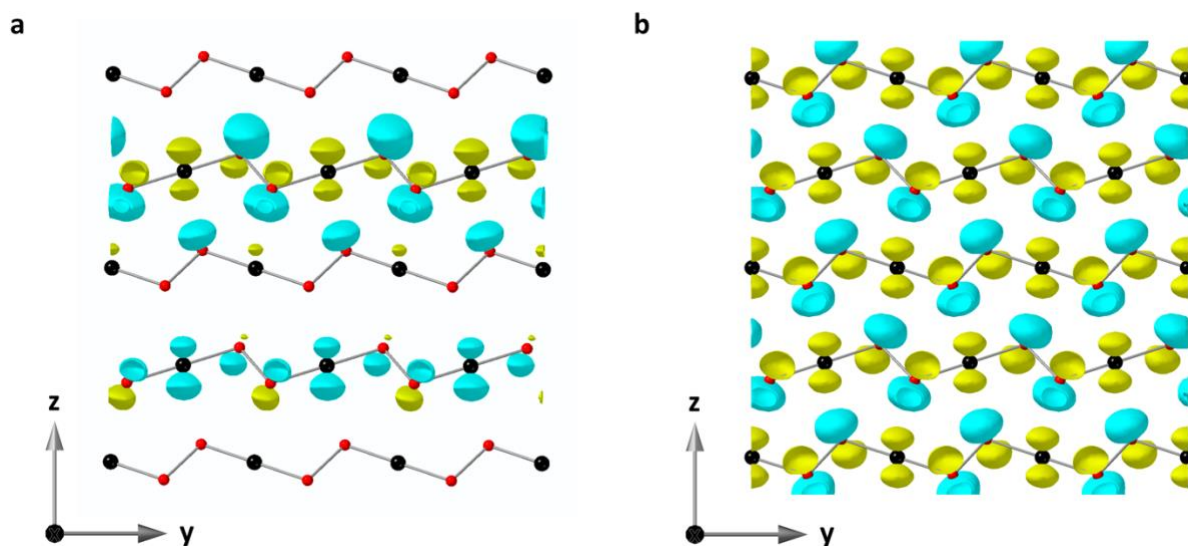


## Supplementary Information for:

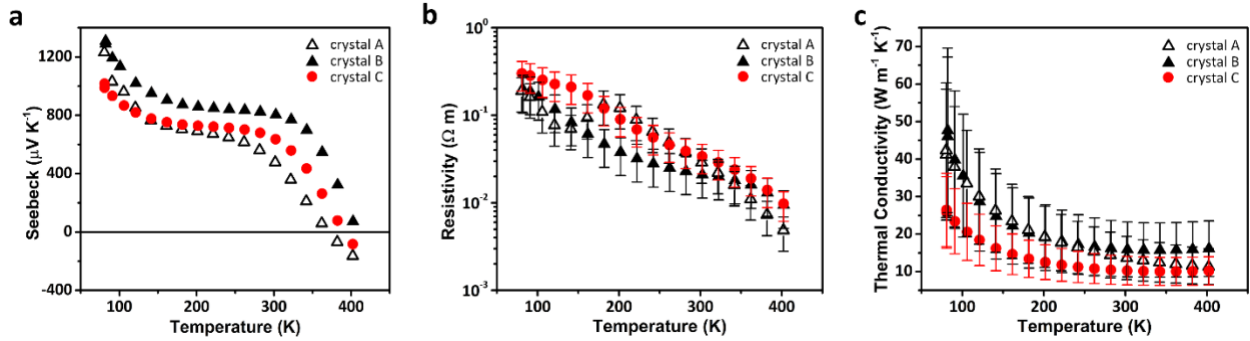
### Axis Dependent Conduction Polarity in the Air-stable Semiconductor, PdSe<sub>2</sub>

Ryan A. Nelson, Ziling Deng, Andrew M. Ochs, Karl G. Koster, Cullen T. Irvine, Joseph P. Heremans, Wolfgang Windl and Joshua E. Goldberger\*

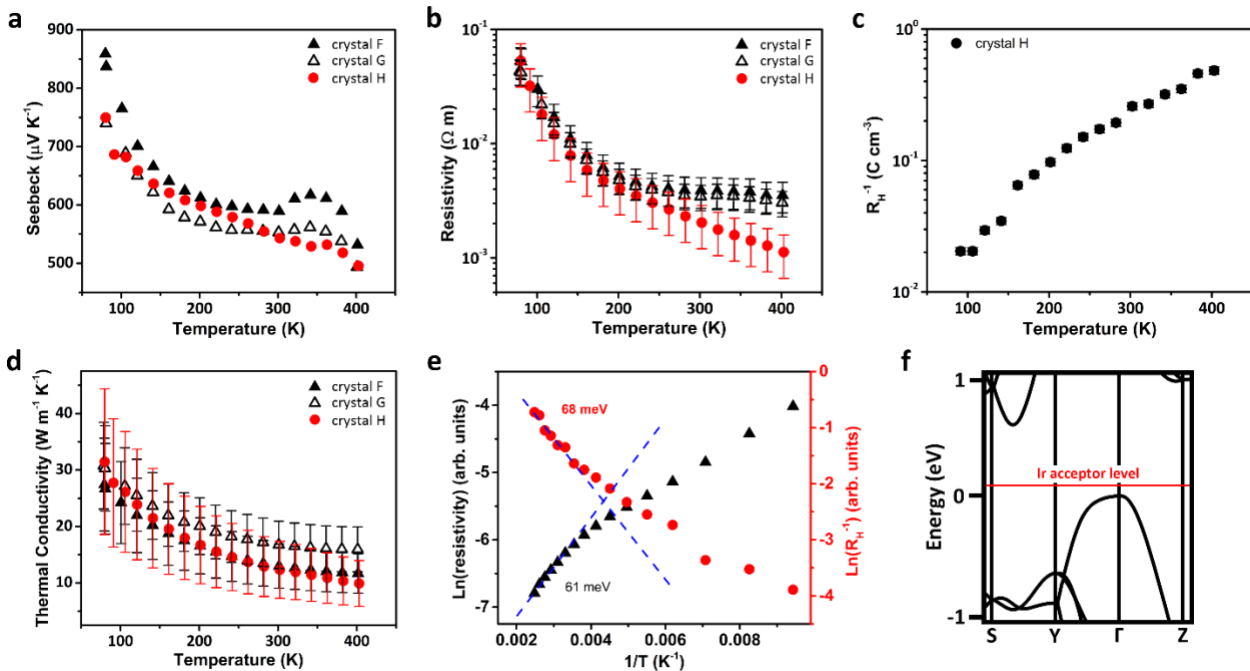
#### Supplementary Figures



**Supplementary 1. Orbital character of the valence band maximum at Z and  $\Gamma$ .** Real component of the wavefunction calculated for the VBM at the **a)** Z point and **b)**  $\Gamma$  point. Only one layer of the yz-plane is shown for clarity. Orbital composition for both points is comprised mainly of Pd  $4d_{z^2}$  and Se  $4p_z$  orbitals. The relatively weak in-plane interactions at Z remain largely unchanged relative to the  $\Gamma$  point. The strong antibonding cross-plane interactions seen at the  $\Gamma$  point are significantly attenuated at Z.



**Supplementary 2. In-plane transport for lightly Ir-doped PdSe<sub>2</sub>.** **a)** In-plane thermopower as a function of temperature for crystal A (from the main text) as well as two other crystals that show the same cross-over behaviour in the range from 350 to 400 K. **b)** In-plane resistivity as a function of temperature for the same three lightly Ir-doped crystals. **c)** In-plane thermal conductivity as a function of temperature for all three crystals.



**Supplementary 3. In-plane transport for heavily Ir-doped PdSe<sub>2</sub>.** **a)** In-plane thermopowers as a function of temperature measured on three different heavily Ir-doped crystals. Note the lack of a cross-over to negative thermopower, even up to 400 K. **b)** In-plane resistivity as a function of temperature measured on the same three crystals. **c)** Measured in-plane inverse Hall coefficient for crystal H. **d)** Temperature dependent thermal conductivity on the same crystals. **e)** The Arrhenius treatment, as discussed in the main text in section 2.4, for resistivity and carrier concentration performed on crystal H. The activation energies extracted from the data are in close agreement and indicate an energy barrier of 61 – 68 meV. **f)** Band structure schematic illustrating the energy level of the Ir acceptors at 61 – 68 meV from (e).

## Estimation of Measurement Errors

### Thermopower

The error in the thermopowers is generally quite small. Theoretically, the magnitude of the error depends only on the uncertainty in the nanovolt meter, as geometric variance is factored out by the formula for Seebeck coefficients. Thus, the relative error in the measurements of thermopower are on the order of <1 %. Specifically, the formula for estimating the error in the thermopower takes the following form,

$$S_{err} = \sqrt{\left(\frac{50 \text{ nV}}{V_{Hot}}\right)^2 + \left(\frac{50 \text{ nV}}{V_{Cold}}\right)^2 + \left(\frac{50 \text{ nV}}{V_{Seebeck}}\right)^2}$$

Where 50 nV is the uncertainty in the nanovolt meter,  $V_{Hot}$  is the hot-side thermocouple voltage,  $V_{Cold}$  is the cold-side thermocouple voltage, and  $V_{Seebeck}$  is the voltage generated by the thermal gradient. The voltages are typically orders of magnitude larger than the 50 nV uncertainty in the nanovolt meter.

### Resistivity

The error in resistivity is a bit more complex since the geometric variances become important. This geometric variance generally dominates the error, especially with more irregular shaped samples. The general formula for estimating the uncertainty in the resistivity measurements takes the form,

$$\rho_{err} = \sqrt{\left(\frac{50 \text{ nV}}{V_{sample}}\right)^2 + \left(\frac{dL}{L}\right)^2 + \left(\frac{dW}{W}\right)^2 + \left(\frac{dTh}{Th}\right)^2}$$

Where  $V_{sample}$  is the voltage measured across the sample,  $dL$  is the variance in the length dimension (distance between thermocouples),  $dW$  is the variance in the width dimension (distance between Hall contacts), and  $dTh$  is the variance in the thickness dimension (remaining dimension on the face of the sample containing the thermocouples). The voltage across the sample is typically much larger than the uncertainty in the nanovoltmeter, but the geometric variance can range from 5% to 50% of a given dimension, especially for thin samples. Very thin samples can lead to variances in the geometry as high as 80%.

### Thermal Conductivity

The error in thermal conductivity is also highly sensitive to the geometric variance and has the form,

$$\kappa_{err} = \sqrt{\left(\frac{50 \text{ nV}}{V_{Hot}}\right)^2 + \left(\frac{50 \text{ nV}}{V_{Cold}}\right)^2 + \left(\frac{dL}{L}\right)^2 + \left(\frac{dW}{W}\right)^2 + \left(\frac{dTh}{Th}\right)^2}$$

Where  $V_{Hot}$  is the hot-side thermocouple voltage,  $V_{Cold}$  is the cold-side thermocouple voltage, and the geometric variances discussed previously hold. Again, the voltages are typically much larger than the nanovolt uncertainty, but the same geometric variances suffered by the resistivity measurements act on the thermal conductivity as well. Thus, the relative error in resistivity is often the same in thermal conductivity.

### Inverse Hall Coefficient ( $1/R_H$ )

The inverse Hall coefficient ( $1/R_H$ ) is plotted because it is proportional to carrier density using a single carrier approximation. The error in the inverse Hall coefficient ( $1/R_{H,err}$ ) is the error in the Hall measurement. The error in the Hall measurement is dependent on geometric variance, but only in one dimension. The error formula is as follows,

$$1/R_{H,err} = \sqrt{\left(\frac{50 \text{ nV}}{V_{Hall}}\right)^2 + \left(\frac{dTh}{Th}\right)^2}$$

Where  $V_{Hall}$  is the Hall voltage measured across the sample and  $dTh$  is, again, the variance in the thickness dimension (on the face of the sample containing the thermocouples, roughly perpendicular to the Hall current). The variance in the thickness dimension is usually relatively small, on the order of 5 – 10%. But irregular geometry and thin samples can push this variance to >50% error.